Pergamon

*Ann. occup. Hyg.*, Vol. 41, No. 3, pp. 249–268, 1997
British Occupational Hygiene Society

Published by Elsevier Science Ltd
Printed in Great Britain
0003-4878/97 $17.00+0.00

PII: S0003-4878(97)00001-X

# ACID LEACHING STUDIES OF CHRYSOTILE ASBESTOS FROM MINES IN THE COALINGA REGION OF CALIFORNIA AND FROM QUEBEC AND BRITISH COLUMBIA

A. Morgan

Biomedical Research, AEA Technology, 551 Harwell, Didcot OX11 ORA, U.K.

(*Received* 20 *September* 1996)

**Abstract**—The dissolution of magnesium (Mg) and silicon (Si) from various samples of chrysotile asbestos was measured in N HCl at 25°C. Nine samples were used, five from Canada and four from the Coalinga deposit in California. With milled samples from Quebec, the fraction of Mg dissolving was linearly related to the square root of the leaching time until at least 65% had dissolved. With a hand-picked sample of ore from Quebec, the sample from British Columbia and all the Californian samples, the Mg leaching patterns were sigmoid. The leaching patterns for Si were sigmoid in shape for all the materials tested. Mean Mg dissolution rates were calculated for each leaching period. Considerable differences were observed between samples from the different mining regions and also between hand-picked and milled samples from the same mine. Initially, Mg dissolved more rapidly from milled Quebec chrysotiles than from the Coalinga samples. This difference is due in part to the rapid dissolution of non-structural brucite, present in all the samples from Quebec but not in those from California. An additional cause is greater damage to the fibre surfaces resulting from the milling to which the less readily-opened fibres, typical of the Quebec mining area, were subjected. Once this readily-available Mg had dissolved, there was little difference in leaching rates between milled and unmilled samples from the different regions. When the fraction of Mg dissolving is plotted against that of Si, all the materials follow a similar pattern, suggesting that the dissolution of Si (as silica) is the rate-controlling step in the dissolution of Mg.


## INTRODUCTION

Chrysotile is the most abundant member of the serpentine class of asbestiform minerals. It is a magnesium silicate with ideal composition $Mg_6Si_4O_{10}(OH)_8$. Structurally, the unit fibrils of chrysotile consist of a 1:1 mixed sheet of silica and brucite ($MgO{\cdot}H_2O$) and, because of a slight structural mismatch in lattice parameters, the sheets form either a helical spiral, or concentric cylinders, about a central capillary. Chrysotile fibres consist of polyfilamentous bundles of unit fibrils with their axes in common alignment. The structure and properties of chrysotile have been reviewed recently by Langer and Nolan (1994).

Chrysotile is readily attacked by both organic acids (Thomassin *et al.*, 1977; Goni *et al.*, 1979) and mineral acids (Atkinson and Rickards, 1971; Morgan *et al.*, 1971b, 1973) and there is considerable evidence that it is also degraded *in vivo* (Morgan *et al.*, 1971a; Morgan, 1994). The acid-leaching characteristics of chrysotile samples from the Coalinga region of California have never been described, and the purpose of this paper was to compare them with materials from mines in Quebec and in British Columbia, for which data already exist. Coalinga fibre was chosen because there is evidence from diverse sources that it differs from most other forms

of chrysotile in ways that are likely to affect its solubility. For example, it has been shown that Coalinga fibre is virtually unique in its geological formation (Coleman, 1957; Mumpton and Thompson, 1975), morphology and ultrastructural appearance (Naumann and Dresher, 1966) and fibre dimensions, both as an aerosol and in aqueous suspension (Pinkerton *et al.*, 1983). Following its administration to experimental animals, its biological effects appear to be less severe than those induced by other types of chrysotile (Pinkerton, 1982; Muhle *et al.*, 1987; Rittinghausen *et al.*, 1990).

Geologically, Coalinga chrysotile occurs within the boundaries of the New Idria ultrabasic intrusive, which was cold-injected from great depths. The resulting dunite-derived serpentine has been subjected to extensive tectonic shearing (Coleman, 1996). This mode of formation is quite different to that which gave rise to the Canadian cross- or slip-fibre veins that were formed at high temperature in the absence of physical shearing. The Coalinga ore, being highly sheared and pulverized, allows high yields of asbestos to be obtained by simple open-pit methods. In contrast, the Canadian ore has to be mined from pits by dynamiting and then crushed and milled to produce a commercial product. Processed Coalinga ore yields a much greater proportion of unit fibrils than the typical long-fibred Canadian product, being uniformly Grade 7 (Woolery and Cohan, 1967). This makes it uniquely suitable for certain commercial applications.

High resolution electron microscopy of chrysotile from Quebec (Yada, 1967) showed that the spaces between adjacent fibrils are filled with amorphous material and, to a large extent, the central pore also. Coalinga chrysotile on the other hand, is characterized by the absence of inter- and intrafibrillar material (Naumann and Dresher, 1966; Chwastiak, 1968). The absence of amorphous material, both between and within the internal pores, has been confirmed theoretically by comparing the distribution functions of surface area versus pore diameter with experimental data (Fripiat and della Faille, 1967) and explains why Coalinga chrysotile is reduced so easily to the fibrillar state. The absence of interfibrillar material should, in theory, make the fibrillar surface of Coalinga chrysotile more accessible to aqueous fluids and therefore increase its solubility.

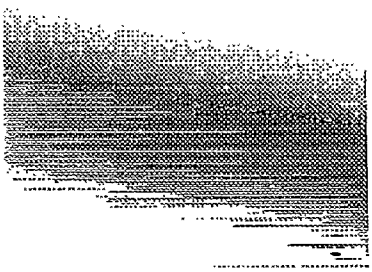

A second factor that might be thought to affect the solubility of chrysotile is fibril diameter. The characteristic diameters of fibrils of Coalinga chrysotile are relatively low, most falling within a narrow range (20–30 nm) with an average of 27 nm (Yada, 1967). Similar values have been reported for Coalinga chrysotile by Naumann and Dresher (1966) who found that fibril diameters for Quebec chrysotiles were much larger, ranging from 20 to over 50 nm with an average of 37.5 nm. The smaller average fibril diameter of Coalinga chrysotile should result in a greater surface area per given weight than for other materials, which should also facilitate dissolution. Indeed, the specific surface areas of Coalinga chrysotile fall within the range 60–68 $m^2\ g^{-1}$ (Chwastiak, 1968) which is three to four times greater than for opened samples from Quebec.

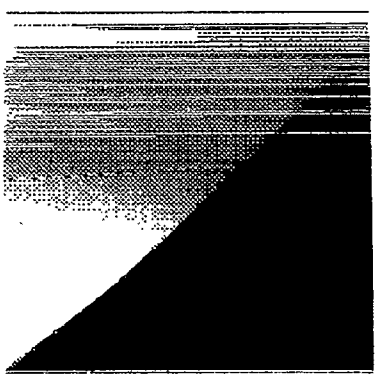

Finally, a third reason for assuming that Coalinga chrysotile should have a high intrinsic solubility is its short fibre length which, combined with the absence of material in the central pores, should permit more rapid dissolution of magnesium from fibre ends. The mean length of Coalinga fibres is about 5 $\mu$m, compared with at least 10 $\mu$m for Quebec samples.

ubility. For example, it has been
geological formation (Coleman,
y and ultrastructural appearance
ons, both as an aerosol and in
ollowing its administration to
r to be less severe than those
n, 1982; Muhle *et al.*, 1987;

the boundaries of the New Idria
eat depths. The resulting dunite-
ve tectonic shearing (Coleman,
to that which gave rise to the
ied at high temperature in the
g highly sheared and pulverized,
y simple open-pit methods. In
n pits by dynamiting and then
t. Processed Coalinga ore yields
e typical long-fibred Canadian
Cohan, 1967). This makes it
ns.
tile from Quebec (Yada, 1967)
filled with amorphous material
a chrysotile on the other hand, is
brillar material (Naumann and
orphous material, both between
theoretically by comparing the
liameter with experimental data
oalinga chrysotile is reduced so
illar material should, in theory,
ore accessible to aqueous fluids

ct the solubility of chrysotile is
rils of Coalinga chrysotile are
(20–30 nm) with an average of
rted for Coalinga chrysotile by
t fibril diameters for Quebec
over 50 nm with an average of
linga chrysotile should result in
er materials, which should also
reas of Coalinga chrysotile fall
) which is three to four times

ga chrysotile should have a high
combined with the absence of
rapid dissolution of magnesium
s is about 5 $\mu$m, compared with

## MATERIALS

### *Chrysotile samples*

Five of the samples used in this study originated from mines in Canada. Of these, the Standard Reference sample B was prepared under the auspices of the Union Internationale Contre le Cancer (UICC) by bulking chrysotile from eight Canadian mines (seven in Quebec and one in British Columbia) roughly in proportion to their annual output. Approximately half the material originated from the Jeffrey mine operated by Johns-Manville. Although it is a mixture of materials, neutron activation techniques have been used to establish that it is homogeneous at the 10 mg level (Morgan and Timbrell, 1971). Additional samples from the Jeffrey mine included a hand-picked sample of unopened ore and two milled samples designated 'Johns-Manville 4-D' and 'Jeffrey 4T-30'. To remove host rock from the hand-picked sample, the fibre ends were removed, leaving fibre bundles about 2 cm in length. Samples of this material for leaching studies were carefully pulled from the fibre bundles to ensure minimal opening. Finally, a very long-fibred silky sample from the Cassiar mine in British Columbia was included.

All the Californian samples were from the Union Carbide mine in the New Idria range. The products designated RG-144 and COF-25 are both of high purity, but the COF-25 material is of even higher purity than the RG-144. The RG-244 material was produced from the COF-25 by treatment with sodium silicate and acetic acid, which results in an amorphous silica coating. The fourth Coalinga sample (designated NIOSH/IITRI CH-29) is one of a range of Analytical Reference Materials prepared by the National Institute for Occupational Safety and Health (NIOSH). Information on its characteristics have been given in reports prepared for NIOSH by Graf *et al.* (1979) and by the IIT Research Institute (Jones and Bock, 1978). It was prepared by grinding a sample of HPO 'Calidria' chrysotile, supplied to NIOSH by Union Carbide, in a centrifugal knife mill. According to Graf *et al.* (1979), fragments of metal introduced during knife milling account for 1–2% of the sample mass. Although it is denser and more granular in appearance than RG-144 chrysotile, it is reputed to have similar properties.

### *Physical properties of the chrysotile samples*

Data on the specific surface areas of six of the samples used in this investigation are given in Table 1. The values for the opened samples from Quebec ranged from 16 to 27 $m^2\ g^{-1}$, whereas those for the Calidria chrysotiles were much greater, as would be anticipated from their different morphology, and fell within a narrow range (54–59 $m^2\ g^{-1}$).

### *Chemical composition of the chrysotile samples*

It is well known that the Mg and Si contents of chrysotile samples are invariably less than indicated by the ideal formula. This is due partly to an excess of $H_2O$ and also to the presence of small amounts of accessory minerals, which can include brucite, calcite, chromite, magnetite, talc and tremolite. In addition, iron, chromium, nickel and cobalt can occur as substitutional cations for magnesium within the structural brucite layer of the fibre (Morgan *et al.*, 1973).

Table 1. Specific surface area measurements of samples of chrysotile used

| Chrysotile | Specific surface area ($m^2/g$) |
|---|---|
| Canadian | |
| UICC B | 25.5*, 27.0† |
| Jeffrey hand-picked | ND |
| Jeffrey JM 4-D | ND |
| Jeffrey 4T-30 | 16.5* |
| IOM Cassiar | 18.7* |
| Californian | |
| NIOSH/IITRI CH-29 | ND |
| RG-144 | 58.2* |
| COF-25 | 59‡, 54.2§ |
| RG-244 | 57.2* |

ND: not determined.
*Rimstidt (personal communication).
†Rendall (1970).
‡Jones and Bock (1978).
§Campbell *et al.* (1980).

In studies of chrysotile dissolution, it is usual to express the fraction of Mg passing into solution as a percentage of the total Mg content of the fibre. Clearly, more accurate values can be obtained by using the actual Mg contents rather than the value derived from the ideal formula. Atkinson and Rickards (1971) indicated that Mg can be totally removed from chrysotile by acid treatment, and acid digestion has been used as the initial stage in the destruction of chrysotile in order to determine its amphibole asbestos content (Addison and Davis, 1990). Therefore, measurements were made of the total Mg content of the nine samples of chrysotile used in the present study by refluxing with 2N HCl for 1 h. Longer refluxing times showed that all the Mg dissolved in the first hour of treatment.

## METHODS

### *Leaching procedure for magnesium and silicon dissolution*

The leaching procedure used was essentially the same as that described by Morgan *et al.* (1971b, 1973). Accurately weighed samples (about 20 mg) of each of the test chrysotiles were transferred to 50-ml screw-cap plastic centrifuge tubes (Falcon). Aliquots (25 ml) of N HCl were added to the tubes and the contents dispersed by vigorous hand shaking for 10 s. The tubes were placed in a constant temperature bath at 25°C and the contents mixed by inversion every few hours. After leaching for predetermined periods, the contents of the tubes were filtered through folded filter papers (Whatman No. 1, diameter 15 cm). Aliquots of the filtrates were collected in plastic vials and analysed for magnesium, silicon and iron by inductively-coupled plasma emission spectrometry (ICP-AES). The shortest leaching time was 2 min. In that case, samples were dispersed in the normal manner, and, after contact with acid for 1.5 min, filtration was started and terminated at 2.5 min. The remaining suspension was discarded. Appropriate blank samples were prepared and analysed with each batch of samples, together with a standard solution

containing 50 $\mu$g ml$^{-1}$ of Mg and 10 $\mu$g ml$^{-1}$ of Si and Fe. The limits of detection by ICP-AES for Mg, Si and Fe are 0.05, 0.03, 0.003 $\mu$g ml$^{-1}$, respectively.

In an attempt to increase the dispersion of the chrysotiles, additional fibre suspensions in N HCl were hand-shaken vigorously for 1 min, after which they were treated in the normal manner.

*Determination of total Mg content*

To determine the total Mg contents of the chrysotiles used, accurately weighed samples (20–30 mg) were refluxed with 25 ml of 2N HCl for 1 h. The resulting suspensions were diluted to 50 ml with distilled water and the siliceous residue removed by filtration. Mg, Si and Fe were determined in the filtrates by ICP-AES, as described above.

## RESULTS

*Chemical composition of chrysotile samples*

The Mg contents of the test chrysotiles are given in Table 2 and varied from 23.7 to 24.8%. There was good agreement between duplicate determinations. These values are lower than the Mg content indicated by the ideal formula for chrysotile (26.3%). Lower values than ideal for Mg are to be expected due to the presence of other cations, either in accessory minerals, or as isomorphous substitutes for structural Mg itself. The Mg contents of the Quebec chrysotiles were generally greater than of the Coalinga, presumably because of higher levels of free brucite ($MgO{\cdot}H_2O$). Brucite levels of 5–7 and 1–2% have been reported by Graf and Bock (1984) for UICC B and Coalinga chrysotile, respectively. The Mg content of brucite (41.7%) is considerably greater than that of ideal chrysotile so that significant levels of free brucite will enhance the Mg content of a fibre. As would be expected, the Mg content of the silica-treated RG-244 chrysotile is somewhat lower than of the COF-25 material from which it was prepared.

When expressed as MgO, the normal manner in which Mg contents are expressed, the values in Table 2 correspond to 39.3–41.1%. MgO concentrations

Table 2. Concentrations of magnesium and iron in chrysotile samples based on concentrations in solutions obtained by refluxing in 2N HCl

| Chrysotile | Magnesium content (%) | Iron content (%) |
|---|---|---|
| Canadian | | |
| UICC B | 24.57 | 2.6 |
| Jeffrey hand-picked | 24.63 | 1.2 |
| Jeffrey JM 4-D | 24.06 | 2.8 |
| Jeffrey 4T-30 | 24.16 | 2.2 |
| IOM Cassiar | 24.76 | 1.2 |
| Californian | | |
| NIOSH/IITRI CH-29 | 24.30 | 1.8 |
| RG-144 | 23.70 | 1.7 |
| COF-25 | 23.88 | 1.4 |
| RG-244 | 21.65 | 1.4 |

Results are the means of duplicate measurements.

| ıples of chrysotile used |
|---|
| ace area ($m^2/g$) |
| *, 27.0† |
| ND |
| ND |
| 6.5* |
| 8.7* |
| ND |
| 8.2* |
| 54.2§ |
| 57.2* |

to express the fraction of Mg
Mg content of the fibre. Clearly,
actual Mg contents rather than
n and Rickards (1971) indicated
e by acid treatment, and acid
struction of chrysotile in order to
on and Davis, 1990). Therefore,
of the nine samples of chrysotile
l for 1 h. Longer refluxing times
of treatment.

olution

the same as that described by
amples (about 20 mg) of each of
rew-cap plastic centrifuge tubes
d to the tubes and the contents
. tubes were placed in a constant
d by inversion every few hours.
ntents of the tubes were filtered
liameter 15 cm). Aliquots of the
for magnesium, silicon and iron
metry (ICP-AES). The shortest
e dispersed in the normal manner,
n was started and terminated at
. Appropriate blank samples were
, together with a standard solution

ranging from 40.8 to 42.8% for chrysotiles derived from serpentine ultramafics have been reported by Langer and Nolan (1994), compared with the ideal value of 43.7%. The Mg contents of a range of 28 cross-fibred chrysotiles have been given by Hahn-Weinheimer and Hirner (1975). The mean value that they obtained was 41.87%, but it should be noted that prior to analysis, their samples were ground and subjected to magnetic separation in order to remove as much free magnetite as possible. This will have enhanced the Mg content.

The iron contents of the samples are included in Table 2 and ranged from 1.2 to 2.8%. According to Langer and Nolan (1994), the iron contents of chrysotile fibres, derived from serpentine ultramafics range from 0.5 to 3.6%. Morgan *et al.* (1973) showed that about half the iron in samples of chrysotile from Quebec is present as magnetite, most of the remainder being substituted for Mg in structural brucite. It is not known whether all the iron in chrysotile is dissolved by refluxing with 2N HCl, but the Fe concentration of the UICC B sample reported here is identical with that previously measured by neutron activation analysis (Morgan and Timbrell, 1971). This suggests that the values obtained by acid refluxing do represent total iron contents. The iron contents of the milled Quebec samples were greater than of the Coalinga. The hand-picked Jeffrey sample had a low iron content (1.2%), which is presumably due to freedom from host rock contamination. The Cassiar sample also had an Fe content of only 1.2% in agreement with previously published values by Morgan *et al.* (1973) and by Martin and Phillips (1977).

The $SiO_2$ content of ideal chrysotile is 43.4%, and values ranging from 38 to 44% have been reported (Rubin and Maggiore, 1974). It was clear from the siliceous residue left after refluxing with 2N HCl, that not all the silica in chrysotile is dissolved by this treatment. The mean weight of Si dissolving after refluxing various amounts of chrysotile with 2N HCl was relatively constant (2.5±0.36 mg), indicating that, on average, only about 10% of the Si had dissolved.

*Dissolution of magnesium*

In Fig. 1(A), the loss of Mg from chrysotile samples from Quebec and British Columbia, expressed as a percentage of their total Mg contents, is plotted against the square root of the leaching times. Where three determinations were made at a single time point, standard deviations are included. It has been shown that, when leaching results are plotted in this manner, the data can be fitted by a straight line until most of the Mg has dissolved (Atkinson and Rickards, 1971). The leaching patterns for the UICC B and milled Quebec chrysotiles all conform to this pattern, following a straight line until at least 60% of the Mg had dissolved. Linear regression lines for these three samples, obtained by fitting all the data up to a Mg dissolution of 65%, are shown in Fig. 1(A) as continuous lines. The correlation coefficients are all greater than 0.99, and the $y$-axis intercepts are 8.0, 2.6 and 2.2% for the UICC B, J-M 4-D and Jeffrey 4T-30 samples, respectively. The pattern for the hand-picked Jeffrey sample has a somewhat different shape: although the curve passes through the origin, only the data obtained between 4 and 100 h approximate to a straight line. The leaching pattern for the Cassiar chrysotile has a linear portion that passes through the origin but then tends upwards rather than downwards. Fig. 1(B) shows that the Mg leaching patterns for the Calidria samples all have a sigmoid

d from serpentine ultramafics have
ared with the ideal value of 43.7%.
ysotiles have been given by Hahn-
at they obtained was 41.87%, but
ples were ground and subjected to
ree magnetite as possible. This will

in Table 2 and ranged from 1.2 to
iron contents of chrysotile fibres,
.5 to 3.6%. Morgan *et al.* (1973)
rysotile from Quebec is present as
d for Mg in structural brucite. It is
solved by refluxing with 2N HCl,
eported here is identical with that
sis (Morgan and Timbrell, 1971).
refluxing do represent total iron
samples were greater than of the
low iron content (1.2%), which is
nination. The Cassiar sample also
th previously published values by
(1977).
, and values ranging from 38 to
74). It was clear from the siliceous
ot all the silica in chrysotile is
dissolving after refluxing various
atively constant (2.5±0.36 mg),
e Si had dissolved.

amples from Quebec and British
l Mg contents, is plotted against
c determinations were made at a
d. It has been shown that, when
ta can be fitted by a straight line
d Rickards, 1971). The leaching
otiles all conform to this pattern.
the Mg had dissolved. Linear
y fitting all the data up to a Mg
ontinuous lines. The correlation
intercepts are 8.0, 2.6 and 2.2%
les, respectively. The pattern for
fferent shape: although the curve
etween 4 and 100 h approximate
iar chrysotile has a linear portion
rds rather than downwards. Fig.
alidria samples all have a sigmoid

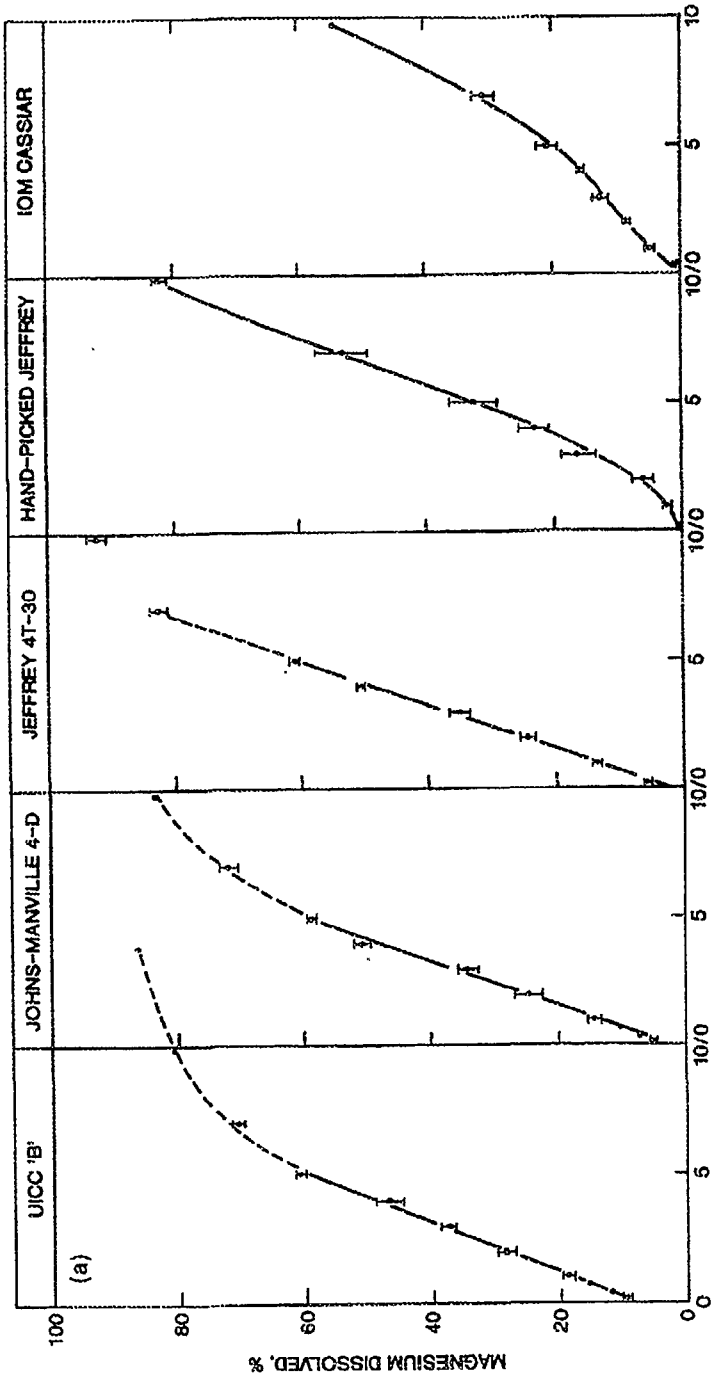


Fig. 1. (A) Magnesium leaching patterns for the Canadian chrysotile samples.

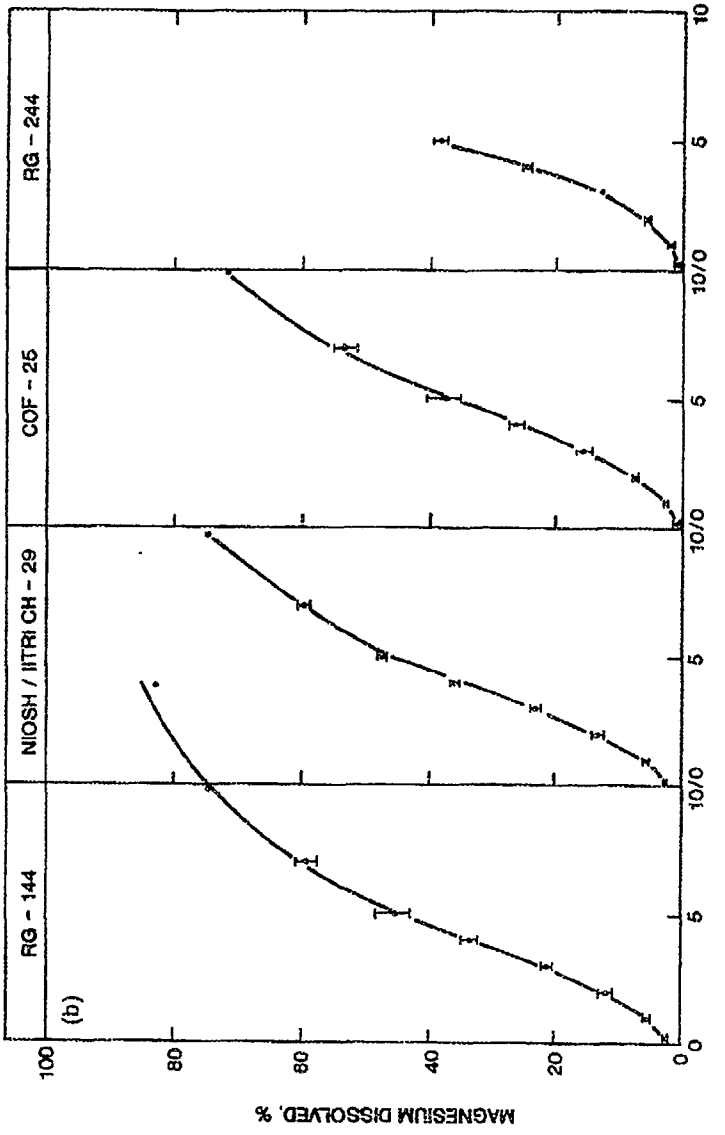


Fig. 1. (B) Magnesium leaching patterns for the Calidria chrysotile samples.

shape. The $y$-axis intercepts are about 2% for the RG-144 and NIOSH/IITRI CH-29 samples and less than 1% for the RG-244 and COF-25 samples.

There was no systematic increase in Mg solubility when the suspensions of chrysotile in acid were shaken for 60 rather than 10 s. This indicates that additional hand-shaking failed to increase the dispersion of the chrysotile samples used.

*Dissolution of silicon*

Data for the dissolution of Si are shown in Fig. 2A and Fig. 2B. The loss of Si is expressed as a percentage of the total Si based on the ideal formula for chrysotile (20.27%). The Si leaching patterns are all sigmoid in shape, irrespective of mining region, and the $y$-axis intercepts are all less than 0.5%.

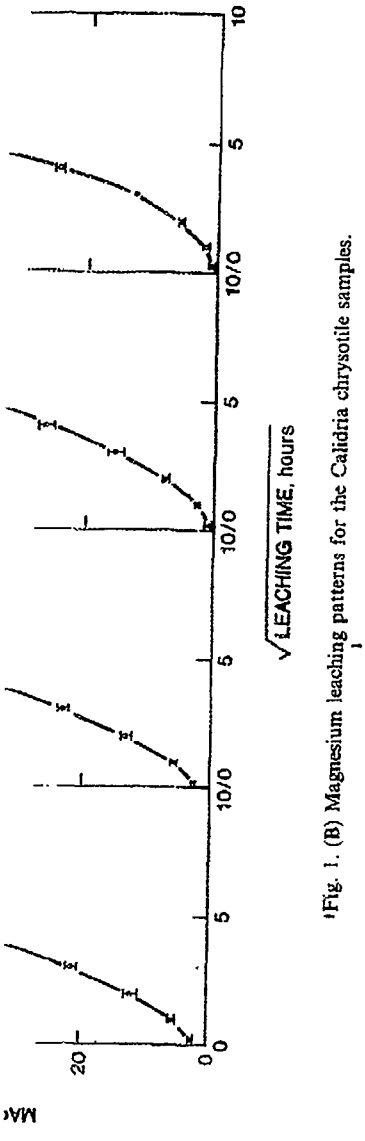


Fig. 1. (B) Magnesium leaching patterns for the Calidria chrysotile samples.

## DISCUSSION

The acid decomposition of chrysotile has been studied by a number of authors. Atkinson and Rickards (1971) showed that the rate of reaction is directly proportional to acid concentration in the range 1–12N. At concentrations lower than this, the rate of reaction decreases more slowly. Dissolution of Mg from a range of chrysotile samples, including UICC B, was investigated by Morgan *et al.* (1971b, 1973) using identical conditions to those in the present study. They showed that the Mg leaching patterns for milled chrysotiles from three Quebec mines (Bells, Normandie and Jeffrey), and for the UICC B standard reference sample, were all linear until about 70% had dissolved and that the $y$-intercepts were in the range 5–10%. The values reported for the UICC B sample are in excellent agreement with those reported here, in respect of both slope and $y$-axis intercept. Thus, it would appear that the leaching patterns of milled chrysotiles from mines in Quebec generally exhibit a linear relationship between the loss of Mg and the square root of the leaching time and have a significant $y$-intercept. However, the leaching pattern of the hand-picked Jeffrey material is quite different and resembles more closely those of the Coalinga chrysotiles that all have similar sigmoid shapes.

Undoubtedly, the higher intercepts for the Quebec chrysotiles are due in part to the rapid dissolution of (a) free brucite, the concentration of which is higher in Quebec than Coalinga samples and (b) interstitial Mg containing material, thought to be amorphous hydrated magnesium silicate (Bates and Comer, 1959), which is present in Quebec chrysotiles and absent in those from Coalinga. Chrysotile from the Carey mine in Quebec, which was reported by Wagner *et al.* (1970) to contain an abnormally high free brucite concentration of at least 20%, gave a very high $y$-intercept of about 35% on acid leaching (Morgan *et al.*, 1973). The free brucite contents of the other components of the UICC B material were reported by Wagner *et al.* (1970) to be either less than 5% or, in the case of the Cassiar component, absent. The low free brucite and iron contents of the Cassiar and Coalinga chrysotiles may not be altogther fortuitous. Both arise along the Pacific rim and may originate from similar starting materials (Coleman, personal communication). Not unexpectedly, the Cassiar fibre also demonstrates a poorly formed and thus rather weak interfibrillar matrix (Martin and Phillips, 1977), no tremolite contamination (O'Hanley, personal communication) and generally exhibits an exceptional purity that gives rise to its preferred use as an electrical insulator (Sinclair, 1955).

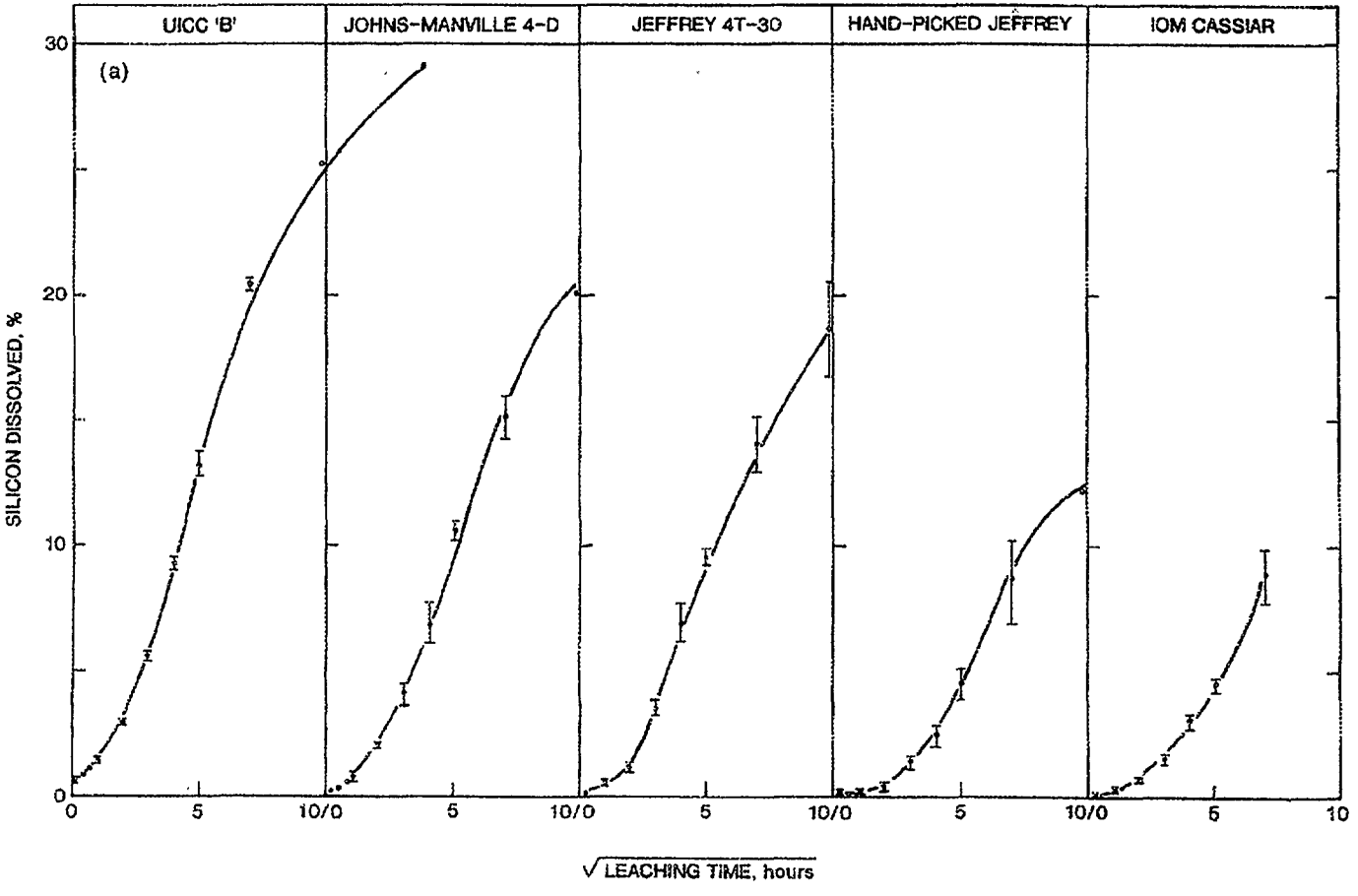


Fig. 2. (A) Silicon leaching patterns for the Canadian chrysotile samples.

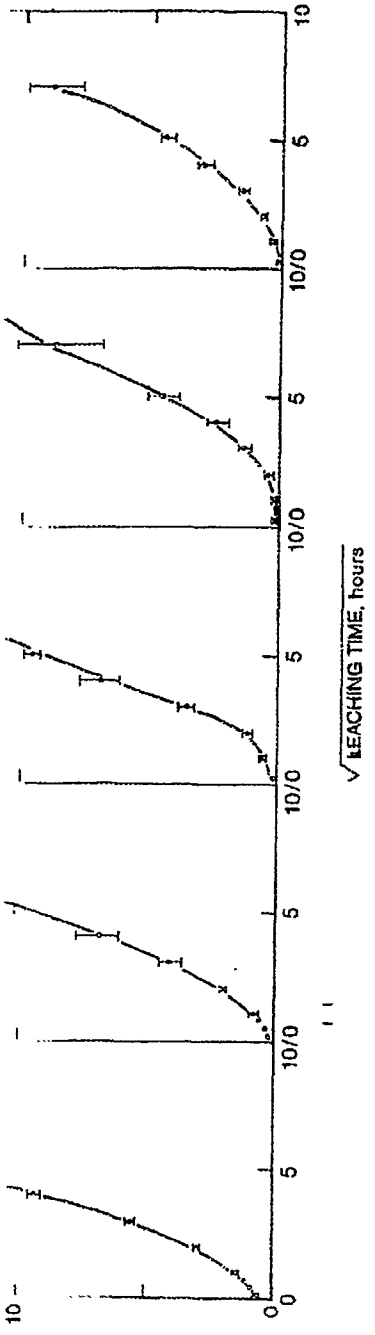


Fig. 2. (A) Silicon leaching patterns for the Canadian chrysotile samples.

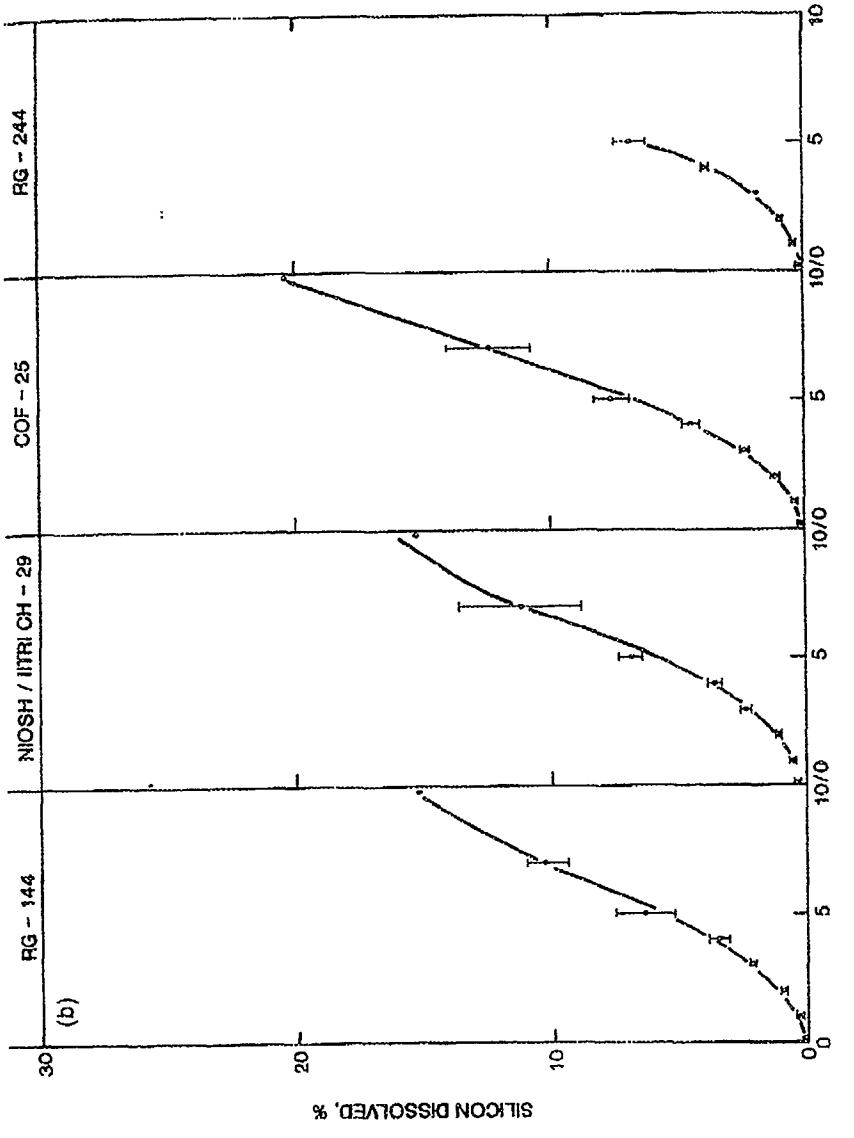


Fig. 2. (B) Silicon leaching patterns for the Calidria chrysotile samples.

Another factor that is known to affect Mg solubility is milling. Mechanical milling of chrysotile is known to decrease fibre crystallinity and alter Si–O and Mg–O interlayer bonding (Langer *et al.*, 1978). The acid leaching characteristics of 'rough' and 'milled' UICC standard reference samples were compared by Morgan *et al.* (1973) who showed that the effect of milling was to increase both the *y*-intercept and the rate of Mg dissolution.

In Fig. 3A, the mean Mg leaching rates from the Canadian chrysotiles during each leaching period are plotted against the fraction of the total Mg remaining undissolved at the start of that period. Corresponding data for the Coalinga samples are shown in Fig. 3B. With all the samples, there is an initial enhanced leaching rate of variable duration followed by a plateau phase, during which leaching rates only decline slowly and are generally within the range 1–2.5% $h^{-1}$. After about 30% of the Mg has been removed, leaching rates start to decline more rapidly and, by the time 50% has been removed, are less than 1% $h^{-1}$ for most samples.

Leaching rates during the initial 2-min period are given in Table 3, together with the fraction of the total Mg dissolving during the rapid leaching phase. The end of the rapid leaching phase is taken as the point at which the leaching rate falls below 2.5% $h^{-1}$. It can be seen from Table 3 that the UICC B chrysotile, and the milled samples from Quebec all follow a similar pattern. The initial leaching rates exceed 100% $h^{-1}$, and more than 20% of the Mg is dissolved during this phase. Some of this loss can be accounted for by the high, rapidly-dissolving free brucite content of these samples but, as free brucite accounts for less than 5% of the Mg (Wagner *et al.*, 1970), other factors are clearly more important. The behaviour of the hand-picked Jeffrey sample is quite different; the initial leaching rate is only 6% $h^{-1}$, and only about 0.2% of the Mg is removed during this phase. Cassiar chrysotile, which contains very little free brucite, also has a low initial leaching rate (16% $h^{-1}$) and thereafter appears to have the lowest Mg dissolution rate of all the samples examined. The initial leaching rates of the Coalinga samples range from 30 to 81% $h^{-1}$ and only a few percent of the Mg is dissolved during the rapid leaching phase. Note the similarity between the RG-144 and NIOSH/IITRI, CH-29 samples. The slightly more rapid dissolution of the latter is probably due to the additional milling that it received.

In Fig. 4A, mean values for the fraction of Mg dissolving during each leaching interval are plotted against the corresponding Si values for the Canadian samples. Corresponding data for the Coalinga samples are shown in Fig. 4B. The relationships so obtained follow a rather similar pattern with a steep initial increase, followed by a gradual turn over. Figure 4A shows that, despite the large difference in 'openness', the curves for the hand-picked and milled samples from the Jeffrey mine are almost identical when plotted in this manner. With the UICC B sample, rather more Si has to be dissolved to achieve the same Mg depletion and even more for the Cassiar. As shown in Fig. 4B, there is a very close similarity between the RG-144 and NIOSH/IITRI CH-29 samples. Rather more Si had to be dissolved from the RG-244, and its parent COF-25, to achieve a comparable Mg dissolution.

Comparing Fig. 4A and 4B shows that, when expressed in this way, the patterns for the Quebec chrysotiles are not dissimilar to the Coalinga. Dissolution of 10% of the Si results in a Mg depletion of 50±10% and dissolution of 20% to a Mg

g solubility is milling. Mechanical
rystallinity and alter Si–O and Mg–
he acid leaching characteristics of
mples were compared by Morgan *et*
was to increase both the *y*-intercept

m the Canadian chrysotiles during
action of the total Mg remaining
ding data for the Coalinga samples
is an initial enhanced leaching rate
e, during which leaching rates only
1–2.5% $h^{-1}$. After about 30% of
o decline more rapidly and, by the
$^{-1}$ for most samples.
are given in Table 3, together with
e rapid leaching phase. The end of
which the leaching rate falls below
UICC B chrysotile, and the milled
. The initial leaching rates exceed
solved during this phase. Some of
y-dissolving free brucite content of
ss than 5% of the Mg (Wagner *et*
iant. The behaviour of the hand-
leaching rate is only 6% $h^{-1}$, and
is phase. Cassiar chrysotile, which
itial leaching rate (16% $h^{-1}$) and
solution rate of all the samples
linga samples range from 30 to
ssolved during the rapid leaching
d NIOSH/IITRI, CH-29 samples.
is probably due to the additional

g dissolving during each leaching
values for the Canadian samples.
are shown in Fig. 4B. The
lar pattern with a steep initial
4A shows that, despite the large
ked and milled samples from the
this manner. With the UICC B
ieve the same Mg depletion and
, there is a very close similarity
mples. Rather more Si had to be
25, to achieve a comparable Mg

pressed in this way, the patterns
Coalinga. Dissolution of 10% of
d dissolution of 20% to a Mg

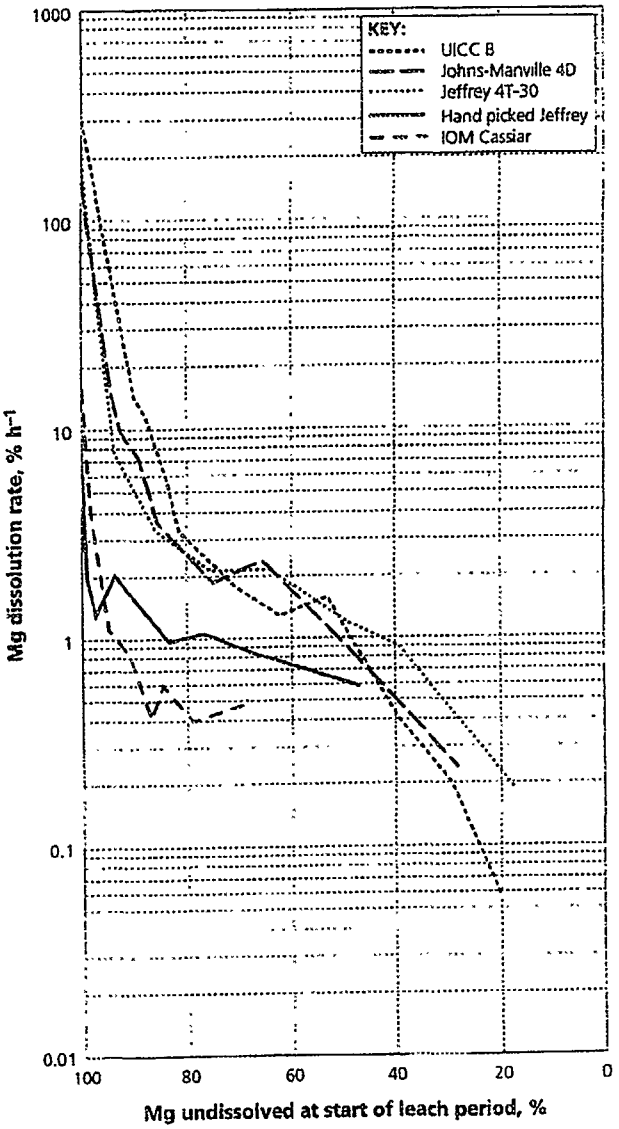


Fig. 3. (A) Magnesium dissolution rates versus the fraction of magnesium undissolved at the start of the leach period. Results for Canadian samples.

dissolution of > 70%. The only exception to this pattern is the Cassiar chrysotile. It would appear therefore, that the removal of Mg from the chrysotiles used in the present study depends primarily on the rate of Si (as silica) dissolution and that this is the rate-controlling factor. These conclusions are in agreement with the 'shrinking fibre' model of Hume and Rimstidt (1992) who proposed that the structural brucite

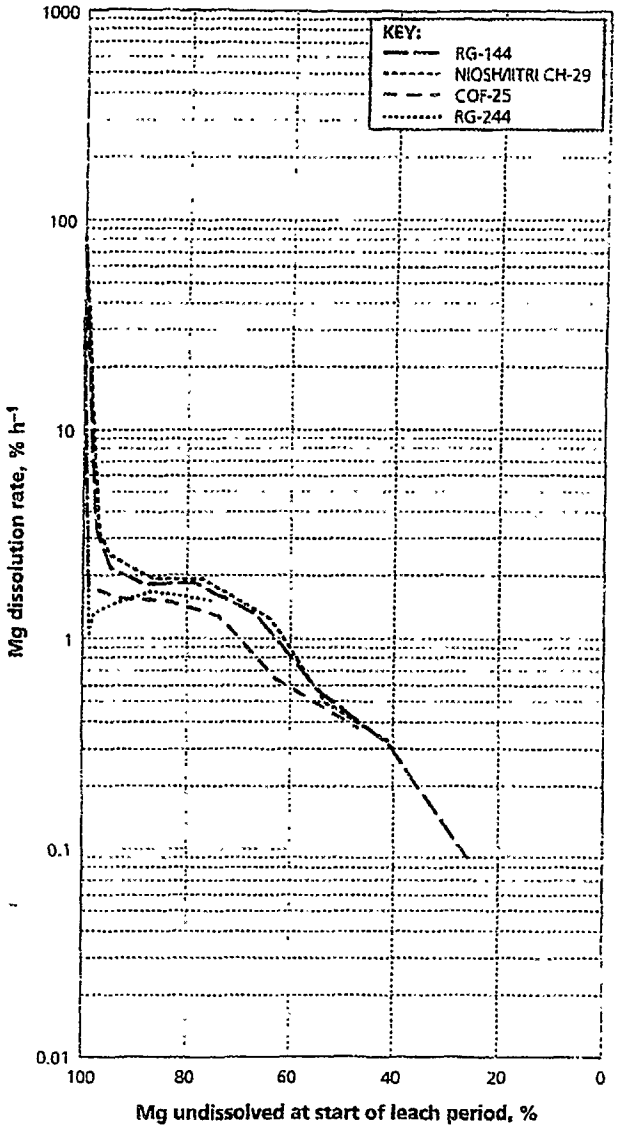


Fig. 3. (B) Results for Calidria samples.

of chrysotile dissolves, thus exposing the silica layer, which dissolves at a lower rate and is thus the rate-controlling step.

If it is assumed that the rapid dissolution of interfibrillar material exposes all the fibril surface to acid, then it might be anticipated that the subsequent leaching rates of Si (and consequently of Mg) would be similar. That they are not, suggests that there are intrinsic differences in the rate of dissolution of the Si. The most likely explanation of this is that damage to the surfaces of Quebec chrysotile fibres, due to

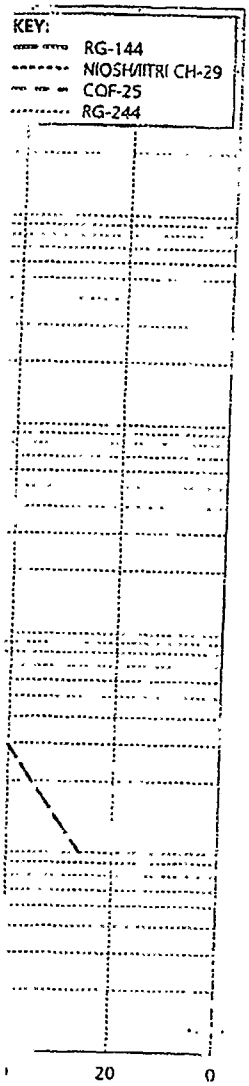


each period, %

ria samples.

yer, which dissolves at a lower rate

terfibrillar material exposes all the
that the subsequent leaching rates
r. That they are not, suggests that
olution of the Si. The most likely
of Quebec chrysotile fibres, due to

Table 3. Initial leaching rates and fraction of magnesium dissolving during rapid leaching phase

| Chrysotile | Initial leaching rate (% $h^{-1}$) | Fraction dissolving (%) |
|---|---|---|
| Canadian | | |
| UICC B | 301 | 23 |
| Jeffrey hand-picked | 6 | 0.2 |
| Jeffrey JM 4-D | 156 | 20 |
| Jeffrey 4T-30 | 179 | 22 |
| IOM Cassiar | 16 | 3 |
| Californian | | |
| NIOSH/IITRI CH-25 | 81 | 6 |
| RG-144 | 71 | 5 |
| COF-25 | 30 | 0.5 |
| RG-244 | 30 | 0.5 |

their more extensive milling, results in a more rapid dissolution of Si than from the relatively undamaged Coalinga fibres. Topographic images of the surfaces of hand-picked and milled (4T-30) Jeffrey samples obtained with an atomic force microscope (AFM) are shown in Fig. 5A and 5B, respectively. Breakage and damage to the fibrils on the surface of the milled fibres can be clearly seen.

Another factor that may affect dissolution rates is fibril morphology. For example, the Si in cylindrical fibrils may dissolve more slowly than from spiral fibrils, resulting in a slower release of Mg. Fibrils having a spiral structure possess a permanent 'ledge' produced by the emergence of the screw dislocation at the surface of the crystal. Such ledges are absent from fibrils with cylindrical layers. As discussed by Veblen and Wylie (1993), surface ledges probably affect dissolution kinetics, and it is probable that their presence on spiral fibrils enhances their dissolution rates compared to those of cylindrical fibrils.

The rate of dissolution of the magnesium from chrysotile has been estimated *in vivo*, following its administration to rats by intrapleural inoculation (Morgan *et al.*, 1971a). It was found that between 25 and 35% of the Mg in Cassiar chrysotile dissolved during the first month after administration, after which the leaching rate was much reduced. Thus, on the basis of the present study, it appears that *in vivo* leaching rates are roughly 200 times slower than the rate of dissolution in N HCl at 25°C. Therefore, it should take about 4.5 months for 50% of the Mg to dissolve from chrysotile fibres *in vivo*. Dissolution rates of this order are not inconsistent with those indicated by the 'shrinking fibre' model of Hume and Rimstidt (1992), which predicted that a chrysotile fibre 1 $\mu$m in diameter will dissolve completely in 9±4.5 months. Dissolution rates of chrysotile fibres within cells have also been calculated by Parry (1985), who found rates that were similar to those observed *in vivo*. Small changes in the values of the Si/Mg ratio in fibres extracted from lung led Churg and DePaoli (1988) to conclude that dissolution of chrysotile must play a very minimal role in chrysotile clearance in humans. However, if it is accepted that the silicon in chrysotile fibres dissolves *in vivo*, albeit more slowly than the magnesium, then there is likely to be an effective upper limit on the value of this ratio.

To summarize, it is clear from this study that Mg dissolution rates from chrysotile are unrelated to their specific surface areas. It also demonstrated that, whereas there are considerable differences in the rates at which Mg is leached

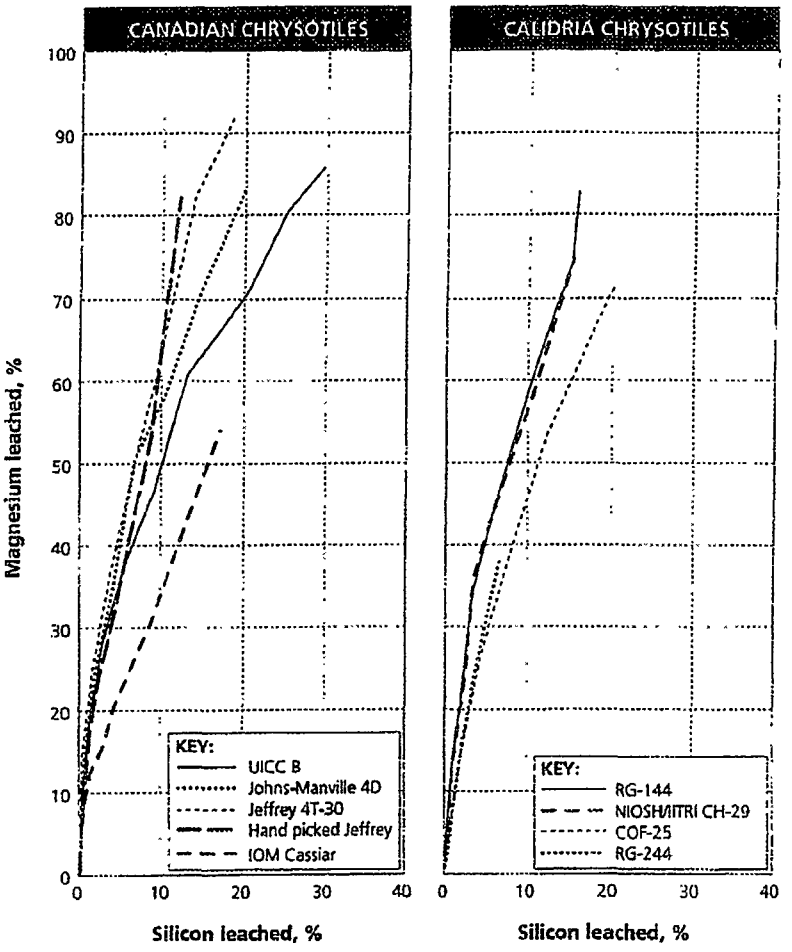


Fig. 4. Fraction of magnesium dissolved versus the fraction of silicon dissolved. (A) Results for Canadian samples. (B) Results for Calidria samples.

from commercial grades of chrysotile from different mining areas, even greater differences exist between hand-picked and milled samples from the same mine. It appears that the rapid initial Mg dissolution rate, which accounts for about 20% of the total Mg in milled samples from Quebec, is due more to damage to fibril surfaces caused by milling than to the relatively high levels of rapidly-dissolving free brucite and interfibrillar magnesium silicates. With the Coalinga chrysotiles, which are opened much more readily, the initial leaching rate accounts for 5% of the total Mg at most. After the initial rapid leaching phase, there appears to be a period during which leaching rates are rather similar for all samples, presumably reflecting Mg removal from exposed and relatively undamaged fibrils below the original fibre surface. During this phase, the dissolution of Mg may be limited by the diffusion of Mg ions through the silicate layer, as suggested by Gronow

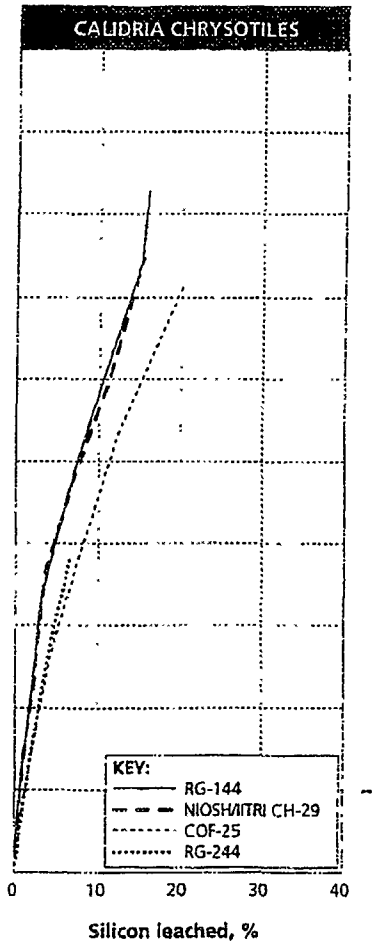


ion of silicon dissolved. (A) Results for Canadian Calidria samples.

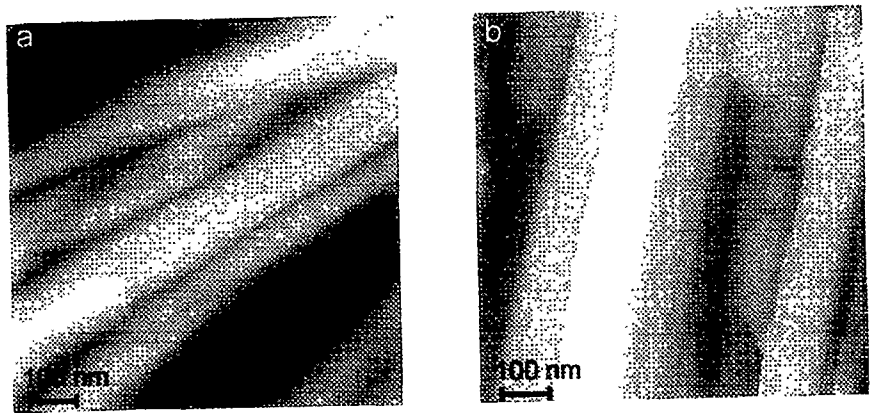


Fig. 5. Atomic force micrographs of (A) hand-picked Jeffrey chrysotile and (B) milled Jeffrey 4T-30 chrysotile.

ı different mining areas, even greater ıilled samples from the same mine. It ı rate, which accounts for about 20% ebec, is due more to damage to fibril ıively high levels of rapidly-dissolving ıicates. With the Coalinga chrysotiles, ıitial leaching rate accounts for 5% of leaching phase, there appears to be a ɔr similar for all samples, presumably ɔlatively undamaged fibrils below the dissolution of Mg may be limited by ɔate layer, as suggested by Gronow

(1987). The dissolution rate of Mg from Cassiar chrysotile appears to be lower than from all the other samples.

In conclusion, this study shows that the physical properties of commercial chrysotiles differ so much that it is impossible to state categorically that the Mg of one dissolves more rapidly than that of another. Differences due to fibril length and diameter, which must affect Mg dissolution rates, are obscured by other factors caused by differences in the treatment of ore necessary to produce a commercial product. Ideally, in order to compare intrinsic leaching rates of chrysotiles, it would be necessary to obtain samples in the fibrillar state without damaging their crystal structure by milling, or other physical treatment. Whereas it is possible that Coalinga chrysotile can be obtained in the fibrillar state, it is unlikely that the same applies to chrysotile from the Quebec mines which are opened much less readily. However, the results presented here suggest that, if absolute fibrillar dissolution rates could be measured for Quebec and Coalinga chrysotiles, they would not be markedly different.

*Acknowledgements*—This investigation was supported by Union Carbide. The author wishes to thank Prof. J. Donald Rimstidt, Virginia Polytechnic Institute, for measurements of specific surface areas, and Dr E. Chatfield, Chatfield Technical Consulting Ltd, who provided some of the samples. Dr Alison Crossley and Dr Carl Sofield, AEA Technology, made the atomic force measurements.

## REFERENCES

Addison, J. and Davis, L. S. T. (1990) Analysis of amphibole asbestos in chrysotile and other minerals. *Ann. occup. Hyg.* **34**, 159–175.

Atkinson, A. W. and Rickards, A. L. (1971) Acid decomposition of highly opened chrysotile. In *Physics and Chemistry of Asbestos Minerals. Second International Conference*, Abstracts of Papers. The University of Louvain, Belgium.

Bates, T. F. and Comer, J. J. (1959) Further observations on the morphology of chrysotile and halloysite. In *Proc. 6th National Conference on Clays and Clay Minerals*, NAS-NRC, pp. 237–248.

Campbell, W. J., Huggins, C. W. and Wylie, A. G. (1980) Chemical and physical charaterization of amosite, chrysotile, crocidolite, and nonfibrous tremolite for oral ingestion studies by the National Institute of Environmental Health Sciences. Report of Investigations 8452. United State Department of the Interior.

Churg, A. and DePaoli, L. (1988) Clearance of chrysotile asbestos from human lung. *Exp. Lung Res.* **14**, 567–574.

Chwastiak, S. (1968) Properties of colloidal chrysotile asbestos from the Coalinga region of California. Union Carbide report.

Coleman, R. G. (1957) Mineralogy and petrology of the New Idria District, California. Ph.D. thesis, Stanford University.

Coleman, R. G. (1996) Tectonic emplacement of the New Idria asbestos-bearing serpentinite: EPA versus BLM land management strategies. *Environ. Engng Geosci.* **2**, 922.

Fripiat, J. J. and della Faille, M. (1967) Surface properties and texture of chrysotiles. *Clays and Clay Minerals, Proc. 15th Conference*, pp. 305–320.

Goni, J., Thomassin, J. H., Jaurand, M. C. and Touray, J. C. (1979) Photoelectric spectroscopy analysis of asbestos dissolution in acidic media of biological interest. In *Origin and Distribution of the Elements*, ed. L. H. Ahrens, pp. 806–817. Pergamon Press, Oxford.

Graf, J. L., Age, P. K. and Draftz, R. G. (1979) *Preparation and Characterization of Analytical Reference Minerals*. U.S. Department of Health Education and Welfare, NIOSH Contract No. 210-75-0043.

Graf, J. L. and Bock, C. (1984) *Investigation of the Feasibility of X-ray Powder Diffraction (XRD) Thin Layer Methods for Screening and Quantitative Analysis of Asbestos*. Final Report on Subcontract No. 8-43U-2069, IITRI Project C06570/C06591, IITRI Research Institute, Chicago.

Gronow, J. R. (1987) The dissolution of asbestos fibres in water. *Clay Miner.* **22**, 21–35.

Hahn-Weinheimer, P. and Hirner, A. (1975) Major and trace elements in Canadian asbestos ore bodies—analytical results and statistical interpretation. *3rd International Asbestos Conference*, Quebec, 1975.

Hume, L. A. and Rimstidt, J. D. (1992) The biodurability of chrysotile asbestos. *Am. Mineral.* **77**, 1125–1128.

Jones, D. and Bock, F. (1978) Characterization of five asbestos mineral fibers. An Addendum to the IITRI Special Report on Project L6085, NIEHS Contract NO. NO1-ES-5-2157.

Langer, A. M. and Nolan, R. P. (1994) Chrysotile: its occurrence and properties as variables controlling biological effects. *Ann. occup. Hyg.* **38**, 427–451.

Langer, A. M., Wolff, M. S., Rohl, A. N. and Selikoff, I. J. (1978) Variation of properties of chrysotile asbestos subjected to milling. *J. Toxic. Environ. Hlth* **4**, 173–188.

Martin, C. J. and Phillips, V. A. (1977) The texture of chrysotile asbestos in relationship to mechanical properties. *Mater. Sci. Engng* **30**, 81–87.

Morgan, A. (1994) The removal of fibres of chrysotile asbestos from lung. *Ann. occup. Hyg.* **38**, 643–646.

Morgan, A., Holmes, A. and Gold, C. (1971a) Studies of the solubility of constituents of chrysotile asbestos *in vivo* using radioactive tracer techniques. *Environ. Res.* **4**, 558–570.

Morgan, A., Holmes, A. and Lally, A.E. (1971b) Solubility of chrysotile asbestos in N hydrochloric acid at 25°C. In *Physics and Chemistry of Asbestos Minerals. Second International Conference*, Abstracts of Papers. The University of Louvain, Belgium.

Morgan, A., Lally, A. E. and Holmes, A. (1973) Some observations on the distribution of trace metals in chrysotile asbestos. *Ann. occup. Hyg.* **16**, 231–240.

Morgan, A. and Timbrell, V. (1971) The use of neutron activation analysis to determine the composition of blended samples of asbestos. *Int. J. appl. Radiat. Isotopes* **22**, 745–751.

Muhle, H., Pott, F., Bellmann, B., Takenaka, S. and Ziem, U. (1987) Inhalation and injection experiments in rats to test the carcinogenicity of MMMF. *Ann. occup. Hyg.* **31**, 755–764.

Mumpton, F. A. and Thompson, C. S. (1975) Mineralogy and origin of the Coalinga asbestos deposit. *Clays Clay Miner.* **23**, 131–143.

Naumann, A. W. and Dresher, W. H. (1966) The morphology of chrysotile asbestos as inferred from nitrogen adsorption data. *Clays Clay Miner.* **23**, 131–143.

Parry, W. T. (1985) Calculated solubility of chrysotile asbestos in physiological systems. *Environ. Res.* **37**, 410–418.

Pinkerton, K. E. (1982) Lung reaction to chronic inhalation of three types of chrysotile asbestos during the lifespan of the Fischer 344 rat. Ph.D. thesis, Duke University.

Pinkerton, K. E., Brody, A. R., McLaurin, D. A., Adkins, B., O'Connor, R. W., Pratt, P. C. and Crapo, J. D. (1983) Characterisation of three types of chrysotile asbestos after aerosolisation. *Environ. Res.* **31**, 32–53.

Rendall, R. E. G. (1970) The data sheets on the chemical and physical properties of the UICC Standard Reference samples. In *Proceedings of the International Conference on Pneumoconiosis, Johannesburg, 1969*, ed. H. A. Shapiro, pp. 23–27. Oxford University Press, Cape Town.

Rittinghausen, S., Ernst, H., Muhle, H., Fuhst, R. and Mohr, U. (1990) Histopathological analysis of tumour types after intraperitoneal injection of mineral fibres in rats. *NATO Workshop on Mechanisms in Fiber Carcinogenesis, Albuquerque*, eds R. C. Brown, J. A. Hoskins and N. F. Johnson, pp. 81–90. Plenum Press, New York.

Rubin, I. B. and Maggiore, C. J. (1974) Elemental analysis of asbestos fibres by means of electron probe techniques. *Environ. Hlth Perspect.* **9**, 81–94.

Sinclair, W. E. (1955) *Asbestos, its Origin, Production and Utilisation*, 2nd edn. Mining Publications, London.

Thomassin, J. H., Goni, J., Baillif, P., Touray, J. C. and Jaurand, M. C. (1977) An XPS study of the dissolution kinetics of chrysotile on 0.1N oxalic acid at different temperatures. *Phys. Chem. Miner.* **1**, 385–398.

Veblen, D. R. and Wylie, A. G. (1993) Mineralogy of amphiboles and 1:1 layer silicates. In *Health Effects of Mineral Dusts*, eds G. D. Guthrie and B. T. Mossman, Reviews in Mineralogy, Vol. 28, pp. 61–137. Mineralogical Society of America, Bookcrafters Inc., Chelsea, MI.

Wagner, J. C., Berry, G. and Timbrell, V. (1970) Mesothelioma in rats following the intrapleural inoculation of asbestos. In *Proceedings of the International Conference on Pneumoconiosis, Johannesburg, 1969*, ed. H. A. Shapiro, pp. 216–219. Oxford University Press, Cape Town.

Woolery, R. and Cohan, W. (1967) New Idria Chrysotile—An unusual ore yields new products. Presentation made at the *4th Joint Conference by the Industrial Minerals Division of the Canadian Institute of Mining and Metallurgy and the American Institute of Mining, Metallurgical and Petroleum Engineers*. Quebec, Canada.

Yada, K. (1967) Study of chrysotile asbestos by a high-resolution electron microscope. *Acta Crystallographica* **23**, 704–707.